UDK 661.852:544.016.2
Original scientific article/Izvirni znanstveni članek

ISSN 1580-2949
Mater. Tehnol.

CHARACTERISATION OF NON-METALLIC INCLUSIONS IN Pb-Ca-Sn ALLOYS

KARAKTERIZACIJA NEKOVINSKIH VKLJUČKOV V ZLITINAH Pb-Ca-Sn

Jožef Medved[1*], Gregor Šegel[2], Tilen Balaško[1], Maja Vončina[1]

[1]University of Ljubljana, Faculty of Natural Sciences and Engineering, Department for Materials and Metallurgy, Aškerčeva 12, 1000 Ljubljana, Slovenia
[2]MPI-reciklaža metalurgija, plastika in inženiring d.o.o., Žerjav 79, 2393 Črna na Koroškem, Slovenia

Prejem rokopisa – received: 2024-02-27; sprejem za objavo – accepted for publication: 2024-01-13

doi:10.17222/mit.2024.1119

Non-metallic inclusions in two Pb-Ca-Sn lead alloys used in the manufacture of lead-acid batteries were investigated and categorised. Samples of recycled lead alloys were analysed using scanning electron microscopy (SEM) in combination with energy dispersive X-ray spectroscopy (EDS). This technique enabled the analysis of the chemical composition of the alloys and the identification of non-metallic inclusions. Differential scanning calorimetry (DSC) confirmed the presence of non-metallic inclusions in two different recycled alloys. Non-metallic inclusions in lead alloys are detrimental, negatively impacting both the casting process and the mechanical and electrochemical properties of the alloys. Results indicate that oxide inclusions are predominant in Pb-Ca-Sn alloys. Non-metallic inclusions with stoichiometric compositions of PbO_2, Pb_2O_3, Al_2O_3, and CaO were identified. Most of these inclusions were found near the surface of a sample, i.e., in the area most exposed to the atmosphere. The introduction of a protective atmosphere during the melting process could significantly reduce the occurrence of non-metallic inclusions.

Keywords: Pb-Ca-Sn alloys, non-metallic inclusions, differential scanning calorimetry

Avtorji v članku predstavljajo raziskavo in kategorizacijo nekovinskih vključkov v dveh svinčevih zlitinah Pb-Ca-Sn, ki se uporabljata za izdelavo kislinskih vžignih akumulatorjev. Vzorce odvzete iz recikliranih svinčevih zlitin so avtorji pregledali z vrstičnim elektronskim mikroskopom (SEM) z uporabo prigrajene energijske difrakcijske spektroskopije (EDS), ki omogoča mikroanalizo kemijske sestave zlitin in vključkov prisotnih v preiskovanih zlitinah. Prisotnost nekovinskih vključkov v dveh različnih recikliranih zlitinah so avtorji potrdili z diferenčno vrstično kalorimetrijo (DSC). Nekovinski vključki, ki se pojavljajo v svinčevih zlitinah, so nezaželeni in negativno vplivajo na potek litja ter mehanske in elektrokemijske lastnosti zlitin. Rezultati kažejo, da se v zlitinah Pb-Ca-Sn nahajajo večinoma oksidni vključki. Identificirani so bili nekovinski vključki s kemijsko sestavo, ki opredeljuje stehiometrijo oksidov PbO_2, Pb_2O_3, Al_2O_3 in CaO. Največ vključkov je bilo prisotnih blizu površine vzorca, ki je imela največ stika z atmosfero. Zagotovo je delež nekovinskih vključkov mogoče znižati z uporabo zaščitne atmosfere med taljenjem.

Ključne besede: zlitine Pb-Ca-Sn, nekovinski vključki, diferenčna vrstična kalorimetrija

1 INTRODUCTION

Lead is the cornerstone of lead-acid batteries, the most common type of rechargeable battery and the preferred power source for most internal combustion engine vehicles. Lead alloys are favoured for their low melting points, ease of processing, cost-effectiveness, good functionality within batteries, and outstanding recyclability.[1] Lead paste and lead grid are the heart of a lead-acid battery, but also the most challenging components to recover during recycling.[2] Traditionally, high-temperature pyrometallurgical processes have dominated the recycling industry. However, significant advancements have been made in recent years to reduce energy consumption, costs, and air pollutant emissions associated with this method.[3–5] While pyrometallurgy remains the primary method for secondary lead recycling, pressure is mounting to develop cleaner and more sustainable alternatives. The traditional smelting method emits lead particles and sulphur oxides, prompting a search for solutions with a lower environmental footprint.[6] The importance of lead recycling is further highlighted by the fact that over half of all lead now comes from secondary sources. Notably, some researchers suggest that secondary lead, primarily derived from recycled lead-acid batteries, has become the main source of this metal in many regions.[7]

Pb-Ca-Sn alloys are the predominant choice in lead-acid batteries, particularly those designed for valve-regulated applications. This popularity stems from their low maintenance requirements, extended service life, and continued performance even during standby periods.[1,8,9] The specific ratio of these alloying elements varies depending on the desired battery characteristics.[9] Among these elements, tin plays a crucial role in enhancing the electrochemical properties of the corrosion layer that forms on the surface of Pb-Sn alloys. This translates to

*Corresponding author's e-mail:
jozef.medved@ntf.uni-lj.si (Jožef Medved)

reduced resistance during battery operation under cyclic loads.[10] Calcium, when added in tiny amounts, significantly strengthens the alloy. Pb-Ca-Sn alloys exhibit excellent precipitation hardening, with the calcium content dictating the proportion of precipitates like $(Pb_{1-x}Sn_x)_3Ca$, $CaSn_3$, and CaSn.[1,11,12] While a powerful deoxidizer, excess calcium can be detrimental as it forms calcium oxides, which compromise both the mechanical and electrochemical properties of the final alloy.[13] Beyond these primary alloying elements, Pb-Ca-Sn alloys boast superior casting properties, enhanced mechanical strength, and optimized electrochemical interactions.[1] However, the presence of impurities like Cu, Sn, Ag, Zn, As, Sb, and Bi in raw lead requires careful control.[14] Managing these impurities is critical for the safe and efficient operation of lead-alloy plants, particularly with respect to corrosion phenomena.[15]

Non-metallic inclusions are compounds formed by the physicochemical reactions between metals and non-metals during metal production, typically during melting or casting processes.[15] Oxides, particularly aluminates, silicates, and spinel inclusions, constitute the majority of inclusions in various metals.[14] Additionally, sulphide and nitride inclusions can form in lead alloys.[16]

Non-metallic inclusions in two distinct Pb-Ca-Sn alloys were investigated using electron microscopy and differential scanning calorimetry (DSC). The analysis aimed to identify, categorize, and characterize these inclusions within the microstructure. DSC analysis confirmed the presence of non-metallic inclusions. A comprehensive understanding of the types of inclusions present in Pb-Ca-Sn alloys can facilitate a deeper insight into their formation mechanisms and contribute to the production of higher-quality alloys.

2 EXPERIMENTAL PART

Two distinct lead alloys, labelled A and B, are essential components in lead-acid battery production. Alloy A, which is characterised by a lower tin content and higher calcium concentration, is employed for the positive pole grid. Conversely, alloy B, which has a higher tin content and a lower calcium concentration, is used for the negative pole grid. Both alloys contain traces of additional elements, but the exact chemical compositions are not disclosed to protect proprietary information.

Samples were extracted from both the centre and the edge of ingots, embedded in epoxy resin, and then polished to a high finish using a BUEHLER EcoMet 30 polishing machine with a series of progressively finer grit papers. Due to the softness of lead alloys, sample preparation required meticulous care. After polishing, the samples were etched for 3–5 s in a 3:1 acetic acid-hydrogen peroxide solution. Given the rapid oxidation of lead surfaces, the samples were examined under a microscope immediately after etching.

Two samples of each alloy were analysed using a Thermo-Fisher Scientific Quattro S FEG-SEM electron microscope equipped with an energy dispersive spectrometer (SEM/EDS) to characterise the inclusions present in the lead alloys.

Differential scanning calorimetry (DSC) was performed using a NETZSCH STA Jupiter 449c. Two samples were extracted from each alloy, A and B: one from the centre of the ingot, where the melt was shielded from the atmosphere during solidification, and another from the edge of the ingot, where the melt was exposed or close to the atmosphere during solidification. An empty corundum crucible served as a reference. Each sample was heated to 400 °C at a rate of 10 $K \cdot min^{-1}$ under a protective argon (Ar 5.0) atmosphere and subsequently cooled to room temperature at the same rate. The resulting DSC heating and cooling curves were used to determine the melting and solidification enthalpies.

3 RESULTS AND DISCUSSION

3.1 Determination of non-metallic inclusions in the investigated Pb-alloys

During the investigation of lead alloys intended for battery grids, several types of non-metallic inclusions were identified. Both alloy samples predominantly contained oxide inclusions. The majority of these inclusions were lead and aluminium oxides, which typically form on a molten metal's surface due to reactions with atmospheric oxygen. Calcium oxide and calcium magnesium oxide were also detected, and categorised as exogenous inclusions. These inclusions are often introduced from external sources, such as contaminants on the surface of molten lead.

In general, inclusions in lead alloys are commonly linked to oxygen exposure, either from the surrounding air or dissolved within the molten metal. A detailed analysis of the identified inclusion types follows.

3.1.1 Lead oxides

Lead oxides (**Figure 1**) primarily form on the surface as oxide scales. During casting, a turbulent flow can cause these scales to sink into the melt. Due to the rapid solidification, they are trapped in the solidified metal matrix. The inclusions observed in **Figures 1a**, **1b**, and **1d** exhibit similar shapes and structures. They all appear to be oxide scales that formed on the melt's surface and were subsequently incorporated into the metal. Lead oxide can also form on a metal's surface during storage and can be incorporated into the melt during remelting. As oxides are brittle, longer oxide scales can fragment. Additionally, lead oxide scales are often associated with porosity.

Figure 1a illustrates a lead oxide layer (spectra 1–5) containing calcium, which is located near the sample's surface. Calcium can significantly degrade the mechanical and electrochemical properties of the lead alloy. **Fig-**

ure 1b, spectrum 1, reveals the presence of PbO_2 inclusions. Similarly, **Figure 1c** shows a PbO_2 inclusion (spectrum 1). The round shape of this inclusion suggests that the surrounding melt solidified first, encapsulating the inclusion. Porosity is evident around the inclusion, likely due to the higher melting point of PbO_2 (290 °C). Spectrum 2, adjacent to the round lead oxide particle, indicates a composition of lead and aluminium oxide, while spectrum 3 consists of lead oxide. In **Figure 1d**, spectrum 1 shows calcium oxide, spectrum 2 indicates sodium oxide, and spectra 3 and 4 show lead oxide.

3.1.2 Aluminates

Aluminium is added to the molten lead to deoxidize the melt prior to the addition of calcium. Aluminium oxide (**Figure 2**) is readily identifiable. Aluminate inclusions and lead oxide can be distinguished primarily by their contrast. Aluminate inclusions appear dark under backscattered electron (BSE) imaging due to their lower density, whereas lead oxides, with a higher density, exhibit a lighter appearance and less contrast with the lead metal. Aluminate inclusions are often found in close proximity to lead oxides, as they are frequently sur-

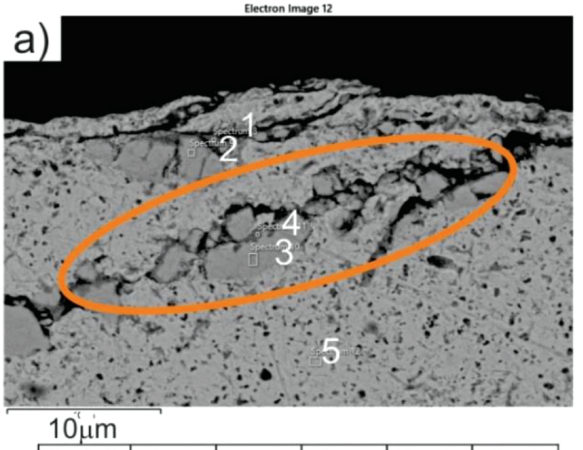

[at/%]	Sp. 1	Sp. 2	Sp. 3	Sp. 4	Sp. 5
O	62.34	50.74	47.95	62.80	31.95
Ca	1.74				
Sn	2.10			1.69	
Pb	33.81	49.26	52.05	35.50	68.05

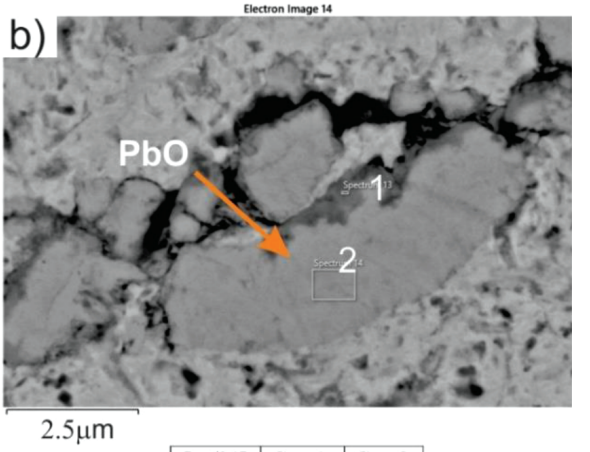

[at/%]	Sp. 1	Sp. 2
O	64.62	47.5
Al	0.91	
Sn	1.15	
Pb	33.33	52.5

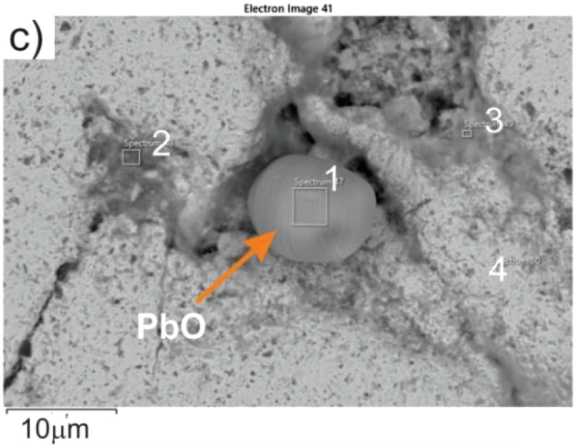

[at/%]	Sp. 1	Sp. 2	Sp. 3	Sp. 4
O	64.96	55.73	67.05	27.26
Al		29.72	6.29	
Pb	35.04	14.55	26.66	72.74

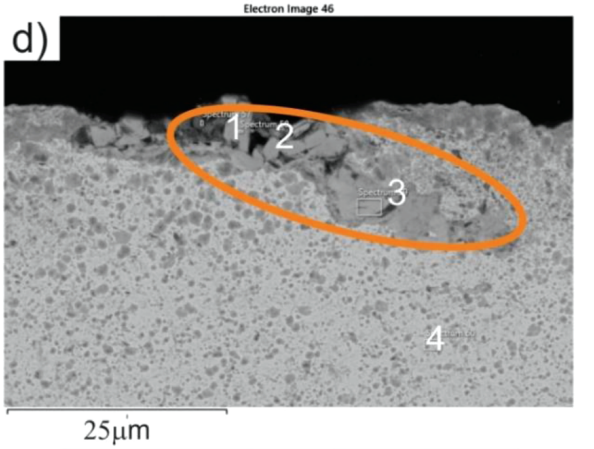

[at/%]	Sp. 1	Sp. 2	Sp. 3	Sp. 4
O	73.11	62.76	58.49	38.83
Na		10.39		
Mg	1.15			
Al	0.47			
Ca	21.12			
Pb	4.15	26.85	41.51	61.17

Figure 1: BSE images of lead oxides in: a) sample A-edge, b) sample B-centre, c) sample A-centre, d) sample B-centre

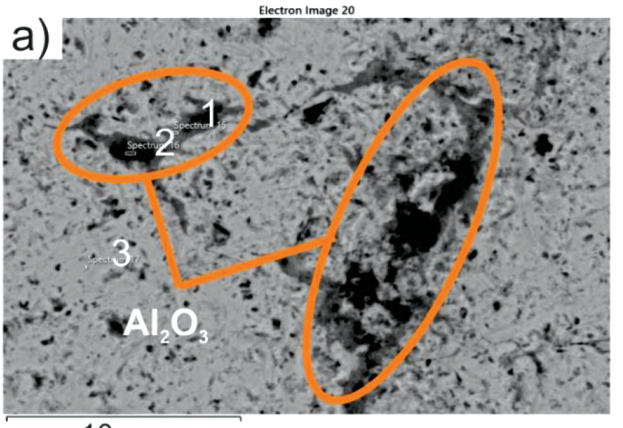

[at/%]	Sp. 1	Sp. 2	Sp. 3
O	63.87	61.89	22.20
Al		29.96	
Sn	1.09		
Pb	35.04	8.15	77.80

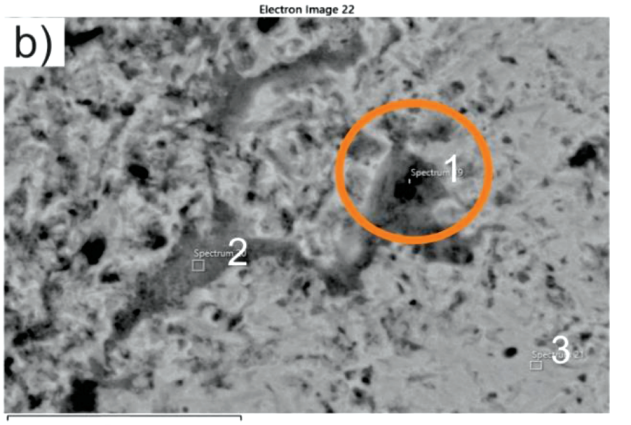

[at/%]	Sp. 1	Sp. 2	Sp. 3
O	63.58	61.90	22.46
Al	16.13		
Sn	0.77	1.10	1.35
Pb	19.52	36.99	76.19

Figure 2: BSE images of aluminates in sample B-centre

rounded by lead oxide. **Figure 2a** depicts an oxide scale, while **Figure 2b** shows lead oxide (spectrum 2) and a combination of lead and aluminium oxide (spectrum 1).

3.2.3 Calcium oxide

Calcium is a crucial alloying element in lead alloys, significantly enhancing their strength properties. As a potent deoxidizing agent, some calcium in the melt oxidizes, forming calcium oxides. **Figures 3a** and **3b** illustrate calcium oxide inclusions (circled in orange) in the alloy microstructure. These inclusions exhibit a spherical shape. Due to their low density, calcium inclusions often congregate on the surface of the melt. In **Figure 3a**, spectrum 1 indicates aluminium oxide, spectrum 2 shows calcium oxide, and spectrum 3 represents lead oxide. In **Figure 3b**, spectrum 1 corresponds to an inclusion composed of calcium and lead oxide, while spectra 2, 3 and 4 represent lead oxide.

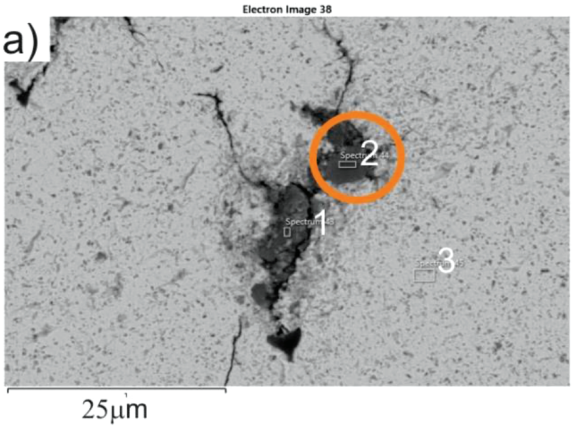

[at/%]	Sp. 1	Sp. 2	Sp. 3
O	61.67	76.47	34.95
Al	37.28	0.30	
Ca		23.03	
Pb	1.05	0.20	65.05

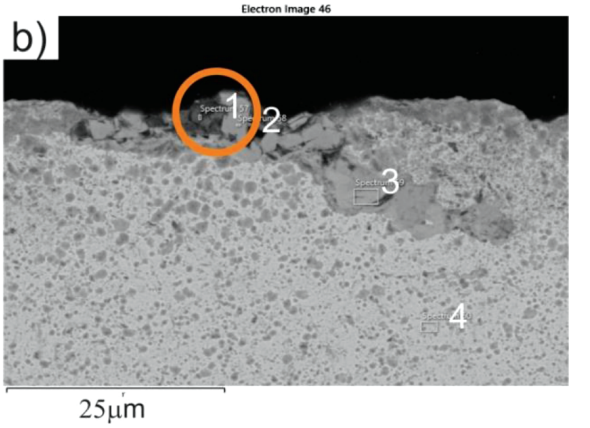

[at/%]	Sp. 1	Sp. 2	Sp. 3	Sp. 4
O	73.11	62.76	58.49	38.83
Na		10.39		
Mg	1.15			
Al	0.47			
Ca	21.12			
Pb	4.15	26.85	41.51	61.17

Figure 3: BSE images of calcium oxide in sample A-edge

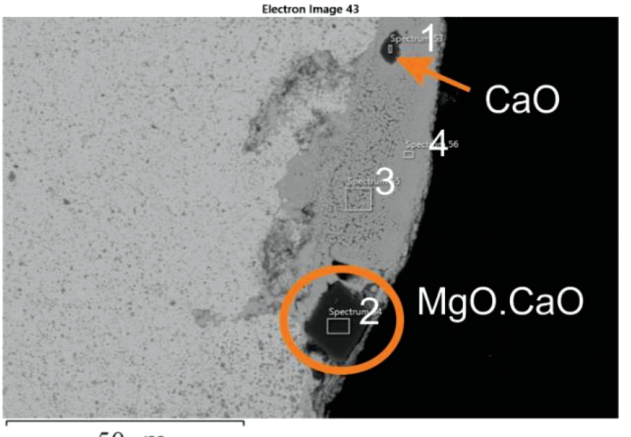

[at/%]	Sp. 1	Sp. 2	Sp. 3	Sp. 4
O	74.07	72.02	70.44	66.30
Mg	0.31	14.04		
Ca	25.13	13.94		
Pb	0.48		29.56	33.70

Figure 4: BSE image of MgO·CaO inclusion in the microstructure of sample A-edge

3.1.4 Calcium magnesite

From the presented data, it can be inferred that the inclusion has a CaO-MgO composition. The calcium magnesite inclusion shown in **Figure 4** is classified as exogenous, as it did not originate from a chemical reaction within the melt but was introduced from an external source. The inclusion exhibits a sharp-edged shape and low density, owing to its composition, and resulting in a distinctly dark appearance. The calcium magnesite inclusion is enveloped by lead oxide, and the structure reveals a calcium oxide inclusion at its apex.

3.2 DSC analysis of investigated Pb-Ca-Sn alloys

DSC analysis confirmed the presence of non-metallic inclusions in the investigated alloys. Samples with lower melting enthalpies show a higher proportion of non-metallic inclusions. The inclusions in the investigated area do not melt, resulting in a lower overall heat requirement for melting and solidification per unit mass. **Figure 5** presents DSC heating and cooling curves of alloy A, relating to both the centre and edge of the ingot. The melting of the centre sample starts at 323.1 °C, corresponding to the melting of the Pb-Sn eutectic (**Figure 5a**). Subsequently, the lead solid solution melts at 333.9 °C. The edge sample exhibits a similar melting onset temperature, although the lead solid solution begins to melt at a slightly lower temperature.

Solidification of both samples starts at 322.5 °C. The lead solid solution solidifies first, followed by the Pb-Sn eutectic at 316 °C and 314 °C, respectively (**Figure 5b**).

The melting and solidification enthalpies of the edge and centre samples of alloy A show negligible differences.

DSC analysis results for alloy B are depicted in **Figure 6**. The melting of the edge sample commences at

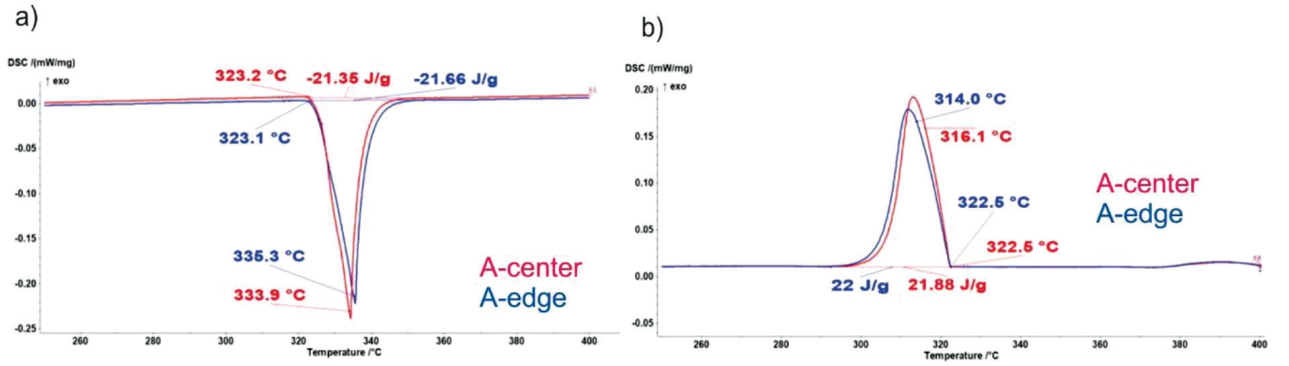

Figure 5: a) Heating and b) cooling DSC curves of alloy A

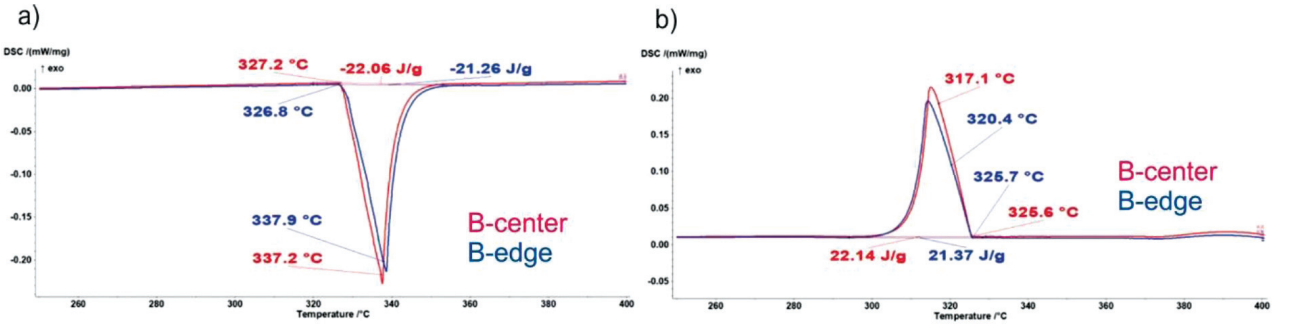

Figure 6: a) Heating and b) cooling DSC curves of alloy B

326.8 °C, corresponding to the melting of the Pb-Sn eutectic (**Figure 6a**). Due to a higher tin content, this eutectic exhibits a lower melting point compared to alloy A. The lead solid solution begins to melt at 337.2 °C. The centre sample of alloy B starts to melt at 327.2 °C, which is 0.4 °C higher than the edge sample's eutectic melting point. The lead solid solution in the centre sample melts at 337.9 °C.

The cooling curves for the edge and centre samples of alloy B are shown in **Figure 6b**. The edge sample's solidification begins at 325.7 °C, followed by Pb-Sn eutectic solidification at 320.4 °C. The centre sample's solidification starts at 325.6 °C, only a tenth of a degree lower than for the edge sample. The Pb-Sn eutectic solidifies at 317.1 °C in the centre sample. Both curves conclude solidification at 290 °C.

In the case of alloy B, the differences in melting and solidification enthalpies are more pronounced. This suggests a higher concentration of inclusions in the alloy with lower melting and solidification enthalpies.

The examination of lead alloys intended for battery grids revealed the presence of various non-metallic inclusions. Both alloy samples were predominantly composed of oxide inclusions. The dominant types were lead and aluminium oxides, which typically form on a molten metal's surface due to reactions with atmospheric oxygen. Additionally, calcium oxide and calcium magnesium oxide were identified. These inclusions are often introduced from external sources, such as contaminants on the surface of molten lead.

4 CONCLUSIONS

The aim of the study was to investigate and categorise non-metallic inclusions in lead battery alloys (Pb-Ca-Sn). These inclusions hinder and complicate the technological process of manufacturing battery grids and shorten their service life. Understanding and preventing the formation of non-metallic inclusions in Pb-Ca-Sn alloys can improve the technological process and product quality.

Based on the results presented, the following can be concluded:

- Oxide inclusions, such as lead oxides (PbO_2, Pb_2O_3), aluminates (Al_2O_3), and calcium oxides (CaO), are the most prevalent in Pb-Ca-Sn alloys. These form during the production of an alloy in the melt. Exogenous inclusions, which mainly originate from magnesite refractories, containing MgO, are also present.
- Inclusions of various compositions often coexist and are closely associated. For instance, aluminium oxide is frequently surrounded by a layer of lead oxide. Porosity is also frequently observed in the vicinity of non-metallic inclusions.
- Non-metallic inclusions can be distinguished by the following characteristics: size (lead oxide forms long oxide scales, whereas aluminate and calcium oxides are usually smaller); shape (inclusions can be sharp-edged, polygonal, spherical, etc.); colour (lower density inclusions are darker); and chemical composition (EDS analysis can be used to examine the chemical composition of samples).
- Both investigated alloys (A and B) exhibit similar solidification patterns: lead solid solutions solidify first, followed by the Pb-Sn eutectic. Characteristic temperatures vary between the alloys due to the differences in the chemical composition. DSC analysis revealed no significant temperature differences between the samples from different parts of the ingot. However, variations in the solidification/melting enthalpy were observed. A lower enthalpy, as seen in sample B-edge, indicates a higher concentration of inclusions in the alloy.

Acknowledgement

We gratefully acknowledge the financial support of the Slovenian Research and Innovation Agency (ARIS) provided under programme grants P2-0344 (B) and P1-0195 (B).

5 REFERENCES

[1] M. T. Wall, M. Carl, J. Smith, Y. Ren, M. Raiford, T. Hesterberg, T. Ellis, M. L. Young, Novel characterization of lead-based micro-alloys for battery applications, Journal of Energy Storage, 44 (**2021**), 103373, doi:10.1016/j.est.2021.103373

[2] T. Liu, K. Qiu, Removing antimony from waste lead storage batteries alloy by vacuum displacement reaction technology, Journal of Hazardous Materials, 347 (**2018**), 334–340, doi:10.1016/j.jhazmat.2018.01.017

[3] B. Chen, J. Cao, F. Ge, J. Zhang, Y. Huang, An innovative synergistic recycling route of spent lead paste and lead grid based on sodium nitrate reuse, Journal of Environmental Chemical Engineering, 10 (**2022**), 108454, doi:10.1016/j.jece.2022.108454

[4] A. D. Ballantyne, J. P. Hallett, D. J. Riley, N. Shah, D. J. Payne, Lead acid battery recycling for the twenty-first century, Royal Society Open Science, 5 (**2018**), 171368, doi:10.1098/rsos.171368

[5] J. Eaves-Rathert, K. Moyer-Vanderburgh, K. Wolfe, M. Zohair, C. L. Pint, Leveraging impurities in recycled lead anodes for sodium-ion batteries, Energy Storage Materials, 53 (**2022**), 552–558, doi:10.1016/j.ensm.2022.08.031

[6] W. Zhang, J. Yang, X. Wua, Y. Hu, W. Yu, J. Wang, J. Dong, M. Li, S. Liang, J. Hu, R. V. Kumar, A critical review on secondary lead recycling technology and its prospect, Renewable and Sustainable Energy Reviews, 61 (**2016**), 108–122, doi:10.1016/j.rser.2016.03.046

[7] T. W. Ellis, A. H. Mirza, The refining of secondary lead for use in advanced lead-acid batteries, Journal of Power Sources, 195 (**2010**), 4525–4529, doi:10.1016/j.jpowsour.2009.12.118

[8] M. M. Burashnikova, I. V. Zotova, I. A. Kazarinov, Pb-Ca-Sn-Ba Grid Alloys for Valve-Regulated Lead Acid Batteries, Engineering, 5 (**2013**), 9–15, DOI: 10.4236/eng.2013.510A002

[9] Y.-B. Zhou, C.-X. Yang, W.-F. Zhou, H.-T. Liu, Comparison of Pb–Sm–Sn and Pb–Ca–Sn alloys for the positive grids in a lead acid battery, Journal of Alloys and Compounds, 365 (**2004**), 108–111, doi:10.1016/S0925-8388(03)00649-2

[10] E. Jullian, L. Albert, J. L. Caillerie, New lead alloys for high-performance lead–acid batteries, Journal of Power Sources, 116 (**2003**), 185–192, doi:10.1016/S0378-7753(02)00705-X

[11] J. P. Hilger, How to decrease overaging in Pb–Ca–Sn alloys?, Journal of Power Sources, 72 (**1998**), 184–188, doi:10.1016/S0378-7753(97)02711-0

[12] X. Yun, F.-Q. Zu, L.-J. Liu, R.-R. Shen, X.-F. Li, Z.-H. Chen, Abnormal solidification of Pb-Sn alloy induced by liquid structure transition, Kovove Materialy, 43 (**2005**), 432–439

[13] Y. Cartigny, J. M. Fiorani, A. Maitre, M. Vilasi, Thermodynamic assessment on the Pb-Ca-Sn ternary system, Intermetallics, 11 (**2003**), 1205–1210, doi:10.1016/S0966-9795(03)00159-6

[14] Z. J. Han, L. Liu, M. Lind, L. Holappa, Mechanism and kinetics of transformation of alumina inclusions by calcium treatment, Acta Metallurgica Sinica (English Letters), 19 (**2006**), 1–8, doi:10.1016/S1006-7191(06)60017-3

[15] J.-L. Courouau, P. Trabuc, G. Laplanche, Ph. Deloffre, P. Taraud, M. Ollivier, R. Adriano, S. Trambaud, Impurities and oxygen control in lead alloys, Journal of Nuclear Materials, 301 (**2002**), 53–59, doi:10.1016/S0022-3115(01)00726-7

[16] J. Burja, M. Koležnik, Š. Župerl, G. Klančnik, Nitrogen and Nitride Non-Metallic Inclusions in Steel, Materials and Technology, 53 (**2019**), 919–928, doi:10.17222/mit.2019.247